




## Thermomagnetic instability of a ferrofluid in a differentially heated Taylor-Couette system

Antoine Meyer , Anupam Hiremath , and Innocent Mutabazi \*

*Normandie Université, UNIHAVRE, CNRS UMR 6294, Laboratoire Ondes et Milieux Complexes (LOMC), 53, rue de Prony, Boîte Postale 540, F-76058 Le Havre Cedex, France*



(Received 22 July 2021; accepted 14 December 2021; published 1 February 2022)

The linear stability analysis of a ferrofluid confined in a cylindrical annulus with a rotating inner cylinder and a resting outer cylinder is performed when a magnetic field and a radial temperature gradient are applied to the ferrofluid. The inhomogeneous magnetic field created by a stack of magnets inserted inside the inner cylinder interacts with the magnetization of the ferrofluid and produces the Kelvin force. The later contains, besides a conservative term, a nonconservative part which can be seen as a magnetic buoyancy with a corresponding magnetic gravity. The magnetic buoyancy generates a thermomagnetic convection in the cylindrical annulus at a critical value of the temperature difference. The threshold of the thermomagnetic convection depends on the radius ratio of the annulus and it is independent of the Prandtl number ( $Pr$ ). The centrifugal instability is affected by the magnetic buoyancy. The centrifugal buoyancy has been included in the analysis and its effects are very sensitive to the diffusive nature of the fluid, i.e., to  $Pr$ . A weak rotation of the inner cylinder decreases the threshold for  $Pr < 325$  and it increases it for  $Pr > 325$ . An energy analysis indicates the relative importance of the dominant mechanisms driving the destabilization of the ferrofluid flow.

DOI: [10.1103/PhysRevFluids.7.023901](https://doi.org/10.1103/PhysRevFluids.7.023901)

### I. INTRODUCTION

A ferrofluid is a nonconducting synthetic stable colloid in which magnetic nanoparticles are suspended in a liquid carrier [1,2]. A surfactant layer on the magnetic particles stabilizes the colloid by preventing them from aggregation. A ferrofluid acts like a paramagnetic material: when an external magnetic field intervenes, the magnetic moments of particles align themselves with the field leading to a finite magnetization which depends on both the applied field and the temperature [3]. The interaction of the magnetic field with the magnetization gives rise to the Kelvin force [3,4].

In the isothermal case, a misalignment of the magnetic field and of the magnetization produces a force which tends to stabilize the flow and can be seen as a source of magnetic viscosity [5]. A sheared flow can lead to such misalignment and for instance can induce the spontaneous rotation of a pipe flow [6]. In particular, the sheared ferrofluidic flow in the Taylor-Couette system has been investigated by many authors for different sources of magnetic fields and different rotation regimes [7–11]. However, in the presence of a temperature gradient, there will be a stratification of the magnetization which leads to the thermomagnetic buoyancy. In most studies [12–18], the magnetization is considered as colinear with the magnetic field. In that case, the magnetic viscosity can be considered with a static magnetization, or it can simply be neglected if the limit where the motion time scale is much longer than the viscous relaxation time of the magnetic nanoparticles is adopted [2,19].

---

\*innocent.mutabazi@univ-lehavre.fr

In addition to the thermomagnetic buoyancy, the centrifugal acceleration acts on the density stratification to produce the centrifugal buoyancy. Depending on the direction of the temperature gradient, this buoyancy may stabilize or destabilize the circular Couette flow. It is found that, both for Rayleigh unstable [20–24] and Rayleigh stable regimes [25–28], the effect of the centrifugal buoyancy increases for fluids with large diffusion properties. An important parameter defined as the temperature drop parameter by Stiles and Kagan [29] or the centrifugal buoyancy parameter by Meyer *et al.* [30] consists of the product of the thermal expansion parameter with the Prandtl number and can successfully characterize the effect of the centrifugal buoyancy in various circular Couette flows.

In this work, we will perform the linear stability analysis of a ferrofluid confined in a differentially heated Taylor-Couette system with applied magnetic field and with a rotating inner cylinder. Since the viscosity of a ferrofluid can take a large range of values (depending on the nature of the carrier), the aim of this analysis is to characterize the role played by the centrifugal buoyancy. In particular, two different values of the Prandtl number corresponding to a water-based and an oil-based ferrofluid will be considered. The present work is an extension of the model derived by Tagg and Weidmann [16] who neglected the contribution of the centrifugal buoyancy and focused their research on fluids with relatively low values of the Prandtl number.

In Sec. II, the theoretical model is derived and the numerical method is introduced. The dependence of the critical parameters on the flow control parameters is presented in Sec. III. In Sec. IV, an energy analysis is performed to highlight the relative importance of the different mechanisms responsible for the change of stability conditions. The behavior of the modes just above the threshold is investigated in the framework of the Ginzburg-Landau analysis in Sec. V. The conclusion is presented in Sec. VI.

## II. PROBLEM FORMULATION

We consider an incompressible ferrofluid with density  $\rho$ , kinematic viscosity  $\nu$ , thermal diffusivity  $\kappa$  and magnetic permeability  $\mu_0$ . The ferrofluid is confined between two coaxial cylinders of infinite length. The inner cylinder of radius  $R_1$  rotates with angular velocity  $\Omega_1$ , while the outer cylinder with radius  $R_2$  is at rest. A temperature difference  $\Delta T = T_1 - T_2$  between the two cylinders is applied, where  $T_1$  and  $T_2$  are the temperatures of the inner and outer cylinder, respectively. A magnetic field  $\mathbf{B}$  is applied within the gap by the integration of a stack of cylindrical magnets inside the inner cylinder (Fig. 1). The stack of magnets has an infinite axial extension, so that the spatial variation of  $\mathbf{B}$  due to the stack ends are neglected. It is assumed that the magnetization  $\mathbf{M}$  of the ferrofluid is in its saturated state and is always aligned with the magnetic field. This assumption holds for ferrofluids with relatively small concentration of magnetic particle, so that the resulting saturated magnetization of the ferrofluid is small. Otherwise, the magnetic field necessary to keep the magnetization in its saturated state would lead to an effect of the thermomagnetic buoyancy so important that the linear stability analysis could not be applicable. Under these assumptions, the Kelvin force density acting on the fluid reads [3]

$$\mathbf{F}_m = \mu_0 M \nabla H. \quad (1)$$

The magnetic field  $\mathbf{H}$  and the magnetic induction  $\mathbf{B}$  are related by a linear relation  $\mathbf{B} = \mu_0(\mathbf{H} + \mathbf{M})$  and they satisfy the current-free magnetostatic Maxwell's equations:

$$\nabla \cdot \mathbf{B} = 0; \quad \nabla \times \mathbf{H} = 0, \quad (2)$$

where  $\mu_0 = 4\pi \times 10^{-7} \text{NA}^{-2}$  is the vacuum permeability. Under the assumption that the magnetization is negligible compared to the magnetic field, it can be expressed that the magnetic induction derives from a magnetic potential  $\phi$ , i.e.,  $\mathbf{B} = -\nabla\phi$ . The equation for the magnetic induction in Eq. (2) results in the Poisson equation for the magnetic potential. In cylindrical coordinates

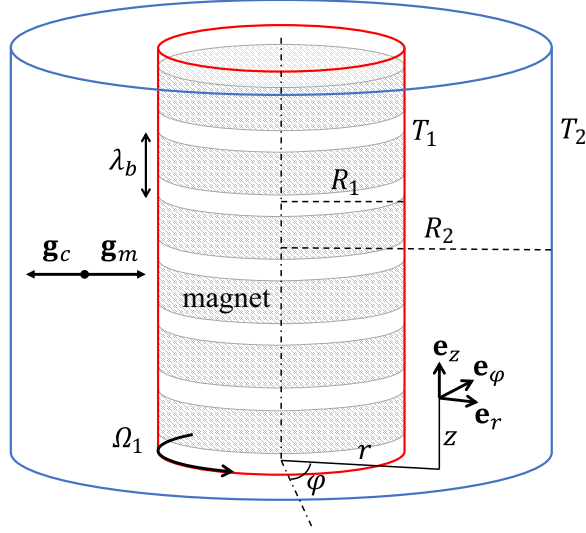


FIG. 1. Schematic representation of the Taylor-Couette system with applied temperature difference and magnetic field due to a stack of magnets located in the inner cylinder.

$(\mathbf{e}_r, \mathbf{e}_\phi, \mathbf{e}_z)$ , the Poisson equation for the scalar axisymmetric magnetic potential reads

$$\frac{\partial^2 \phi}{\partial r^2} + \frac{1}{r} \frac{\partial \phi}{\partial r} + \frac{\partial^2 \phi}{\partial z^2} = 0. \quad (3)$$

The magnetic potential includes an axial periodicity due to the periodicity of the magnets stacked in the inner cylinder. The bounded solution for  $\phi$  is given by

$$\phi = \phi_0 K_0(k_b r) \sin(k_b z), \quad (4)$$

where  $K_0$  is the zeroth order modified Bessel function of second kind and  $k_b = 2\pi/\lambda_b$  is the wave number characterizing the spacing between the magnets (see Fig. 1). The magnitude of the magnetic induction is then given by Ref. [16]

$$B = B_0 K_0(k_b r) \sqrt{1 + \left[ \left( \frac{K_1(k_b r)}{K_0(k_b r)} \right)^2 - 1 \right] \sin^2(k_b z)}. \quad (5)$$

We can see in Eq. (5) that if the quantity under the brackets is small compared to unity, the magnetic induction reduces to  $B = B_0 K_0(k_b r)$ , and the axial dependency vanishes. Taking  $\lambda_b = 3.54d$ , which is the value used by Tagg and Weidmann [16] in connection with experiments, there is a variation along the axial direction of 10% maximum for  $\eta = R_1/R_2 = 0.75$ . This percentage of variation diminishes when  $\eta$  increases and diminishes with the radial distance so that the axial dependence of the magnetic field can be ignored.

The density of the ferrofluid, and therefore its magnetization, decreases with the temperature. For relatively small temperature deviation  $\theta = T - T_2$  from the reference temperature  $T_2$  and at temperature  $T$  below the Curie point, which is the case of most ferrofluids, the density and the magnetization can be expressed using the linear functions of the temperature  $\rho = \rho_{\text{ref}}(1 - \alpha\theta)$  and  $M = M_{\text{ref}}(1 - \alpha_m\theta)$ , respectively, where  $\alpha$  is the thermal expansion coefficient [14,16,17].  $\rho_{\text{ref}}$  and  $M_{\text{ref}}$  are the density and the saturated magnetization of the ferrofluid at the temperature  $T_2$ . The coefficient of thermal variation of magnetization  $\alpha_m$  takes positive values of the order of  $10^{-4}\text{K}^{-1}$  to  $10^{-2}\text{K}^{-1}$  [31]. The Kelvin force (1) now reads

$$\mathbf{F}_m = \nabla[M_{\text{ref}}B_0K_0(k_b r)] + \alpha_m M_{\text{ref}}B_0k_b K_1(k_b r)\theta \mathbf{e}_r. \quad (6)$$

The conservative part of the Kevin force is included into the pressure gradient of the Navier-Stokes equations. The nonconservative part corresponds to the thermomagnetic buoyancy and can be written as  $-\alpha \rho_{\text{ref}} \theta \mathbf{g}_m$  to highlight the analogy with the thermal buoyancy. The magnetic gravity  $\mathbf{g}_m$  is given by

$$\mathbf{g}_m = -g_m \mathbf{e}_r \quad \text{with} \quad g_m = \frac{\alpha_m M_{\text{ref}} B_0 k_b K_1(k_b r)}{\alpha \rho_{\text{ref}}}. \quad (7)$$

The magnetic gravity is centripetal and decreases with the radial distance. Since the saturated magnetization of a ferrofluid can be very large, the resulting magnetic gravity felt inside the gap can be several times larger than that of the terrestrial gravity  $g$ . Indeed, for  $\rho_{\text{ref}} = 1.4 \times 10^3 \text{ kg/m}^3$ ,  $\alpha = \alpha_m = 10^{-3} \text{ K}^{-1}$ ,  $B_0 = 524 \text{ T}$ ,  $M_{\text{ref}} = 10^4 \text{ A/m}$ ,  $d = 3 \times 10^{-3} \text{ m}$  and  $\eta = 0.8$ , we obtain  $g_m = 35g$  at the midgap. The value of the coefficient  $B_0$  leads to a magnetic induction of  $0.2 \text{ T}$  at the inner cylinder, which is sufficient to ensure that the magnetization is in its saturated state.

In the present study, the influence of the terrestrial gravity and consequently the Archimedean buoyancy are neglected. However, an additional thermal buoyancy will act on the flow. Indeed, the rotation of the inner cylinder induces the centrifugal acceleration  $\mathbf{g}_c = (v^2/r) \mathbf{e}_r$ , where  $v$  is the azimuthal component of the velocity. This acceleration interacts with the density stratification to produce the centrifugal buoyancy. The total resulting buoyancy force acting on the ferrofluid is  $\mathbf{C} = \alpha \theta (g_m - v^2/r) \mathbf{e}_r$ . The centrifugal buoyancy and the thermomagnetic buoyancy always act in opposite directions, i.e., depending on the heating direction, when one tends to destabilize the flow, the other tends to stabilize it.

The velocity  $\mathbf{u} = (u, v, w)$ , the pressure  $\pi$ , and the temperature deviation  $\theta$  satisfy the continuity equation, the Navier-Stokes equations and the energy equation

$$\nabla \cdot \mathbf{u} = 0, \quad (8a)$$

$$\frac{\partial \mathbf{u}}{\partial t} + (\mathbf{u} \cdot \nabla) \mathbf{u} = -\nabla \pi + \nu \Delta \mathbf{u} + \mathbf{C}, \quad (8b)$$

$$\frac{\partial \theta}{\partial t} + (\mathbf{u} \cdot \nabla) \theta = \kappa \Delta \theta. \quad (8c)$$

In the energy equation, besides the viscous dissipation term, we have also neglected the term containing the coupling between the temperature and the variation of the magnetic field intensity [12,32,33]. Imposing no-slip conditions at the cylinder surfaces, the boundary conditions read

$$\mathbf{u} = R_1 \Omega_1 \mathbf{e}_\varphi; \quad \theta = \Delta T; \quad \text{at} \quad r = R_1, \quad (9a)$$

$$\mathbf{u} = 0; \quad \theta = 0; \quad \text{at} \quad r = R_2. \quad (9b)$$

Using the gap size  $d = R_2 - R_1$ , the viscous time  $\tau_v = d^2/\nu$ , the pressure  $(\nu/d)^2$  and the temperature difference  $\Delta T$  as characteristic length, time, pressure and temperature, the governing equations (8) read in dimensionless form as

$$\nabla \cdot \mathbf{u} = 0, \quad (10a)$$

$$\frac{\partial \mathbf{u}}{\partial t} + (\mathbf{u} \cdot \nabla) \mathbf{u} = -\nabla \pi + \Delta \mathbf{u} - \gamma_a \frac{v^2}{r} \theta \mathbf{e}_r + \frac{\text{Ra}_m}{\text{Pr}} \frac{K_1(k_b r)}{K_1(k_b \bar{R})} \theta \mathbf{e}_r, \quad (10b)$$

$$\frac{\partial \theta}{\partial t} + (\mathbf{u} \cdot \nabla) \theta = \frac{1}{\text{Pr}} \Delta \theta, \quad (10c)$$

where we introduced the Prandtl number  $\text{Pr} = \nu/\kappa$  and the dimensionless thermal expansion parameter  $\gamma_a = \alpha \Delta T$ . The magnetic Rayleigh number  $\text{Ra}_m = \alpha \Delta T g_m(\bar{R}) d^3/\nu \kappa$  is defined at the midgap position  $\bar{R} = (1 + \eta)/[2(1 - \eta)]$ . We introduced the radius ratio  $\eta = R_1/R_2$  and the Taylor number  $\text{Ta} = \text{Re} \sqrt{d/\bar{R}}$ , where  $\text{Re} = R_1 \Omega_1 d/\nu$ , is defined with respect to the inner cylinder velocity.

The boundary conditions (9) written in dimensionless form read

$$\mathbf{u} = \text{Re}\mathbf{e}_\varphi; \quad \theta = 1; \quad \text{at } r = \eta/(1 - \eta), \quad (11a)$$

$$\mathbf{u} = \mathbf{0}; \quad \theta = 0; \quad \text{at } r = 1/(1 - \eta). \quad (11b)$$

Seeking for a steady, axisymmetric and axially invariant solution, we find the base state which only depends on the radial position

$$\Theta = \frac{\ln[(1 - \eta)r]}{\ln \eta}, \quad (12a)$$

$$V = r\Omega = \frac{\text{Ta}\eta^{3/2}}{(1 - \eta)^{5/2}(1 + \eta)} \left[ \frac{1}{r} - (1 - \eta)^2 r \right], \quad (12b)$$

where  $\Theta$  is the temperature,  $V$  is the azimuthal velocity and  $\Omega$  is the local angular velocity of the base flow. The velocity and the temperature fields are decoupled in the base flow. The temperature gradient is negative, and the heating direction is indicated by the sign of  $\gamma_a$ : the system is in outward heating when  $\gamma_a > 0$  and is in inward heating when  $\gamma_a < 0$ .

We add infinitesimal perturbations to the base state and linearize the resulting equations around the base state. These perturbations are expanded in normal modes  $(u', v', w', \pi', \theta') = (\hat{u}, \hat{v}, \hat{w}, \hat{\pi}, \hat{\theta}) \exp[st + in\varphi + ikz] + \text{c.c.}$ , where *c.c.* stands for complex conjugate. The primed and hatted quantities indicate the perturbation fields and their complex amplitudes, respectively. The time evolution of perturbations is characterized by their complex growth rate  $s = \sigma - i\omega$ , where  $\sigma$  is the temporal growth rate and where  $\omega$  is the frequency. The axial wave number  $k$  is a real positive quantity since the cylinders are of infinite length. The azimuthal mode number  $n$  takes only integer values. We introduce the total wave number  $q = \sqrt{k^2 + k_\varphi^2}$  where  $k_\varphi = 2n(1 - \eta)/(1 + \eta)$  is the azimuthal wave number determined at the midgap. The resulting equations for the complex amplitudes of perturbations are

$$\frac{1}{r}D(r\hat{u}) + \frac{in}{r}\hat{v} + ik\hat{w} = 0, \quad (13a)$$

$$(s + in\Omega)\hat{u} - 2\Omega\hat{v} = -D\hat{\pi} + \Delta\hat{u} - \frac{\hat{u}}{r^2} - \frac{2in}{r^2}\hat{v} + \frac{\text{Ra}_m}{\text{Pr}}\hat{\theta} - \gamma_a(r\Omega^2\hat{\theta} + 2\Theta\Omega\hat{v}), \quad (13b)$$

$$(s + in\Omega)\hat{v} + \left( \frac{d\Omega}{d \ln r} \right)\hat{u} = -\frac{in}{r}\hat{\pi} + \Delta\hat{v} - \frac{\hat{v}}{r^2} + \frac{2in}{r^2}\hat{u}, \quad (13c)$$

$$(s + in\Omega)\hat{w} = -ik\hat{\pi} + \Delta\hat{w}, \quad (13d)$$

$$(s + in\Omega)\hat{\theta} + (D\Theta)\hat{u} = \frac{1}{\text{Pr}}\Delta\hat{\theta}, \quad (13e)$$

where  $D = d/dr$ ,  $\Delta = D^2 + D/r - n^2/r^2 - k^2$ . The perturbations satisfy homogeneous boundary conditions on the cylinder surfaces:

$$\hat{u} = \hat{v} = \hat{w} = \hat{\theta} = 0, \quad \text{at } r = \eta/(1 - \eta); 1/(1 - \eta). \quad (14)$$

The two last terms in the right-hand-side of Eq. (13b) represent the perturbed thermomagnetic buoyancy and the perturbed centrifugal buoyancy. The centrifugal buoyancy includes the effect of the base centrifugal acceleration on the perturbed density profile and the effect of the perturbed centrifugal acceleration on the base density profile. In contrast, the thermomagnetic buoyancy consists only of the effect of the magnetic gravity on the perturbed temperature. Indeed the perturbations of magnetization are neglected compared to the base state one. This approach is justified when thermomagnetic convections are considered in a cylindrical annulus since, in that case, the magnetic field gradient responsible for the Kelvin force is mainly originated by the annulus curvature, and not by the thermal aspect.

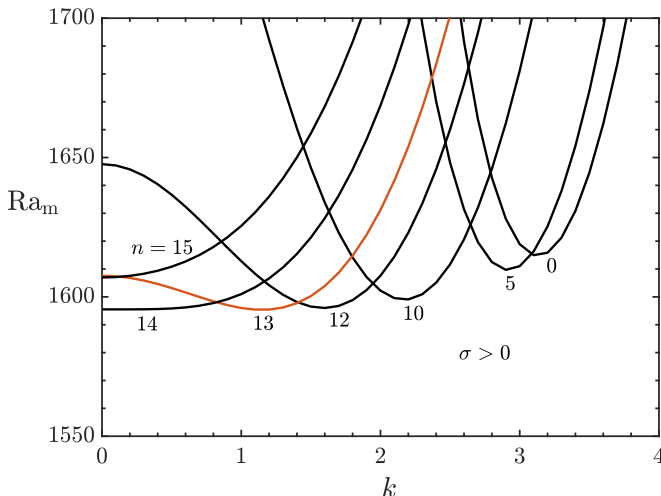


FIG. 2. Magnetic Rayleigh number as function of the axial wave number  $k$  at the marginal state ( $\sigma = 0$ ) for  $\eta = 0.8$ ,  $\text{Pr} = 15$ ,  $\gamma_a = 0.01$ ,  $\text{Ta} = 0$  and for various values of  $n$ . The red curves represents the marginal curve of the critical state which gives the critical parameters  $\text{Ra}_{m,c} = 1595.6$ ,  $k_c = 1.149$ ,  $n_c = 13$  and  $\omega_c = 0$ .

The equations for the complex amplitudes (13) are discretized using the Chebyshev spectral collocation method and completed by the boundary conditions (14). The order of considered Chebyshev polynomials was set to 30 to ensure the convergence of calculations. The resulting generalized eigenvalue problem, written in the matrix form, was solved by the QZ decomposition [34]. Solving numerically the eigenvalue problem gives us eigenvalues  $s$  for a given set of parameters ( $\eta$ ,  $\text{Pr}$ ,  $k_b$ ,  $\gamma_a$ ,  $\text{Ta}$ ,  $\text{Ra}_m$ ,  $n$ ,  $k$ ). A marginal stability state is obtained when the eigenvalue with the largest real part changes the sign from negative to positive values. Marginal stability curves are either plotted in the  $(k, \text{Ta})$  plane for a given set of control parameters ( $\eta$ ,  $\text{Pr}$ ,  $k_b$ ,  $\gamma_a$ ,  $\text{Ra}_m$ ) or in the  $(k, \text{Ra}_m)$  plane for a given set of control parameters ( $\eta$ ,  $\text{Pr}$ ,  $k_b$ ,  $\gamma_a$ ,  $\text{Ta}$ ). The global minimum of marginal stability curves obtained for different azimuthal wave numbers  $n$  gives us the critical conditions ( $\text{Ta}_c$ ,  $n_c$ ,  $k_c$ ,  $\omega_c$ ) for a given  $\text{Ra}_m$  or the critical conditions ( $\text{Ra}_{m,c}$ ,  $n_c$ ,  $k_c$ ,  $\omega_c$ ) for a given  $\text{Ta}$ .

### III. CRITICAL PARAMETERS

Under microgravity conditions, and in the absence of the cylinder rotation, thermomagnetic convections in a cylindrical annulus have been found to be nonaxisymmetric. In particular, the numerical and experimental researches carried out by Polevikov and Fertman [35], Odenbach [36], and Morimoto *et al.* [37] showed the occurrence of counter-rotating pairs of vortices along the azimuthal direction with vortices of about the gap size. The spiral modes have been found by Tagg and Weidman [16] in the case of very low rotation rate of the inner cylinder and when the Earth's gravity can be neglected compared to the magnetic gravity. Figure 2 shows the marginal stability curves obtained for several azimuthal mode number and for  $\eta = 0.8$ . The helical nature of the critical mode is confirmed since the global minimum of the marginal stability curves is obtained for  $n_c \neq 0$  and  $k_c \neq 0$ . The helical vortices are stationary ( $\omega_c = 0$ ) and their critical parameters depend on the radius ratio, but are independent from the Prandtl number. It is worth highlighting the fact that the selection of helical critical modes was also found when the motion of a fluid due to a central force field was analyzed in a cylindrical annulus under microgravity conditions. Alonzo *et al.* [38,39] and Pino *et al.* [40] found such modes while implementing a constant artificial centripetal

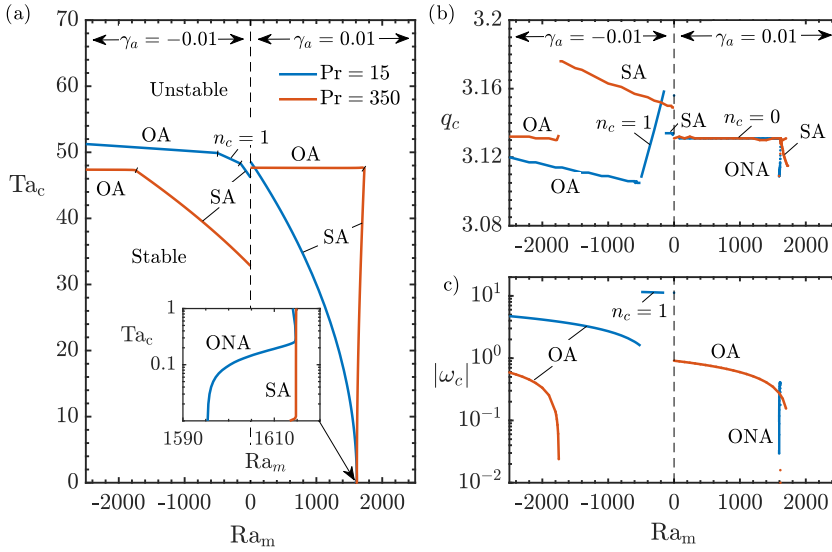


FIG. 3. Variation of (a) the critical magnetic Rayleigh number  $Ra_{m,c}$ , (b) the critical wave number  $q_c$  and (c) the critical frequency  $\omega_c$  with the Taylor number  $Ta$  with  $\eta = 0.8$  and  $|\gamma_a| = 0.01$ .

gravity field for various values of  $\eta$  and  $Pr$ . Similar results were found when a dielectric fluid is subject to the thermoelectric buoyancy associated with an centripetal electric gravity [41–43].

In the absence of magnetic field, the isothermal circular Couette flow with only the inner cylinder rotating is linearly unstable. Above a certain critical Taylor number, the base flow destabilizes to counter-rotating axisymmetric (toroidal) vortices. The critical value of the Taylor number depends only on the radius ratio  $\eta$ . When a radial temperature gradient is applied, the one-dimensional model derived by Meyer *et al.* [30] demonstrated that the centrifugal buoyancy has a stabilizing effect on the Couette flow when  $\gamma_a > 0$  and destabilizes the flow when  $\gamma_a < 0$ . Independently of its stabilizing or destabilizing configuration, the effect of the centrifugal buoyancy is improved by the increase of the thermal expansion parameter and of the Prandtl number [24].

In the presence of a magnetic field, the effect of the thermomagnetic buoyancy on the non-isothermal Taylor Couette system can be evaluated. Figure 3 shows the variation of the critical parameters as functions of the magnetic Rayleigh number for a water-based ( $Pr = 15$ ) and a oil-based ( $Pr = 350$ ) ferrofluid. The different curves are discontinuous at  $Ra_m = 0$  because of the discontinuous change of value of  $\gamma_a$ . In outward heating  $\gamma_a = 0.01$ , for  $Pr = 15$ , the helical modes are stationary for  $Ta = 0$ , and are oscillatory for  $Ta > 0$ . The value of  $n_c$  of these oscillatory nonaxisymmetric (ONA) modes progressively decreases with  $Ta$  from its value with no rotation ( $n_c = 13$ ) to  $n_c = 0$ , however the total wave number increases with the increase of  $Ra_m$  [Fig. 3(b)]. The critical frequency of the ONA modes increases with the magnetic Rayleigh number [Fig. 3(c)]. As shown in Fig. 4, the azimuthal phase velocity  $c_\varphi = \omega/k_\varphi$  of the ONA modes is proportional to the Taylor number. The proportionality between  $c_\varphi$  and  $Ta$  indicates that the rotation of the inner cylinder transports the nonaxisymmetric vortices and brings about the modes oscillation. The critical modes are then stationary axisymmetric (SA). The value of  $Ta$  at the codimension-2 point between ONA and SA modes decreases with increasing  $Pr$  and we determined that for  $Pr = 350$ , the ONA modes become SA at  $Ta = 0.01$ , which implies that the domain of existence of these ONA modes gets negligible for ferrofluids with sufficiently large viscosity.

For  $Pr = 15$ , the critical magnetic Rayleigh number of SA modes decreases with increasing  $Ta$  until it reaches  $Ra_{m,c} = 0$  at the value of  $Ta$  corresponding to the nonisothermal Taylor-Couette instability, which is found to be slightly helical for these values of  $\gamma_a$  and  $Pr$  [24]. The corresponding

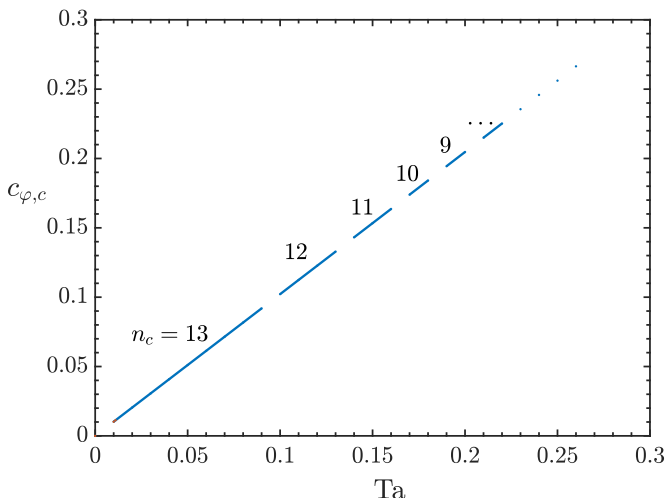


FIG. 4. Behavior of the critical azimuthal phase velocity  $c_{\varphi,c}$  of the ONA modes with respect to  $Ta$  and with  $\eta = 0.8$ ,  $\gamma_a = 0.01$  and  $Pr = 15$ .

critical axial wave number is nearly independent of  $Ta$ . For  $Pr = 350$ ,  $Ra_{m,c}$  for SA modes increases with  $Ta$ . The associated total wave number  $q_c$  decreases with the increase of  $Ra_m$ . At certain value of  $Ta$ , the SA modes become oscillatory axisymmetric (OA) modes. The critical values of Taylor number and wave number of the OA modes are independent of the magnetic Rayleigh number, however their frequency decreases with the increase of the magnetic Rayleigh number. The origin of these oscillations comes from the stabilizing effect of the centrifugal buoyancy in outward heating configurations. At  $Ra_{m,c} = 0$ , the circular Couette flow with heated inner cylinder destabilizes to oscillatory axisymmetric modes if the Prandtl number is sufficiently large. This result was already discussed by Meyer *et al.* [24]. The radial density stratification is stable with respect to the centrifugal buoyancy. The oscillation of modes is therefore excited by the centrifugal buoyancy with a frequency related to the Brunt-Väisälä frequency associated with the centrifugal acceleration. Therefore when the magnetic Rayleigh number increases, the critical frequency diminishes. From Fig. 3(a), we can see that the Taylor number is independent of  $Ra_{m,c}$  for these OA modes, which means that the influence of the centrifugal buoyancy is unchanged with the variation of  $Ra_m$ . However the amplitude of the magnetic gravity increases with  $Ra_m$  leading to the decrease of the Brunt-Väisälä frequency associated with the sum of the centrifugal acceleration and of the magnetic gravity. This result has also been observed by Yoshikawa *et al.* [44] in the case of a dielectric fluid subject to the dielectrophoretic force.

In inward heating ( $\gamma_a < 0$ ), the centrifugal buoyancy plays a destabilizing role which can be observed in Fig. 3(a) through the decrease of  $Ta_c$  with  $Pr$ . In the absence of magnetic field, the critical modes are stationary axisymmetric (SA). The threshold  $Ta_c$  of these SA modes increases with the increase of the magnetic Rayleigh number, indicating the stabilizing effect of the thermomagnetic buoyancy. For sufficiently large values of  $(-Ra_m)$ , the flow destabilizes through the occurrence of OA modes. For  $Pr = 15$  the critical Taylor number of OA modes continues to increase with  $(-Ra_m)$  while for  $Pr = 350$ , the threshold of OA modes is nearly independent of  $(-Ra_m)$ . For  $Pr = 15$ , oscillatory helical modes become critical between the SA and OA modes and over a short range of Rayleigh numbers. These modes, also found in Ref. [44] in the case of thermoelectric convection, are characterized by small number of modes in the azimuthal direction. The wave number [Fig. 3(b)] of SA modes and of OA modes slightly increases with increasing  $Ra_m$  with a discontinuity at the codimension-2 point between these two modes. The wave number of the helical modes occurring for  $Pr = 15$  decreases with the increase of  $Ra_m$ . The frequency [Fig. 3(b)] of OA modes and



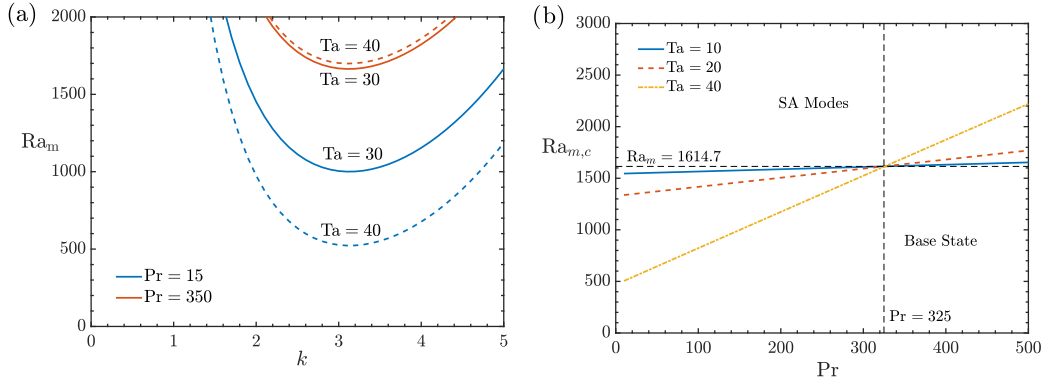


FIG. 5. (a) Magnetic Rayleigh number as function of the axial wave number  $k$  at the marginal state ( $\sigma = 0$ ) and (b) variation of  $Ra_{m,c}$  with  $Pr$ . The parameters are  $\eta = 0.8$ ,  $\gamma_a = 0.01$  and  $n = 0$ .

of helical modes increases with increasing ( $-Ra_m$ ). For sufficiently large values of ( $-Ra_m$ ), the frequency of OA modes tends to be proportional to the root mean square of the magnetic Rayleigh number. This result is similar to what was obtained in Ref. [44] for a dielectric fluid subject to the dielectrophoretic force. The frequency then relates to the Brunt-Väisälä frequency, due to the magnetic gravity acting on the stably stratified density of the fluid and which sustains the oscillation of a perturbation. Figure 5(a) shows the effect of the Taylor number on the marginal stability curves depending on the Prandtl number in outward heating. For a water-based ferrofluid ( $Pr = 15$ ), increasing the Taylor number diminishes the magnetic Rayleigh number at the marginal state. The destabilization of the circular Couette flow is increased by the rotation due to the distribution of angular momentum when only the inner cylinder rotates. However, for an oil-based ferrofluid with  $Pr = 350$ , the Taylor number has the opposite effect on  $Ra_m$  at the marginal state. In that case the centrifugal buoyancy plays an important stabilizing role that overcomes the classical Taylor-Couette destabilization mechanism. The value of  $Pr$  has a major influence on the flow stability since it may impact the role played by the rotation of the inner cylinder.

The effect of the Prandtl number on the threshold of the SA modes is evaluated to better capture the dual role that the rotation of the inner cylinder has on the flow stability. At fixed values of the Taylor number ( $Ta = 10; 20; 40$ ) the variation of the magnetic Rayleigh number with the Prandtl number is calculated and shown in Fig. 5(b). For a given  $Ta$ ,  $Ra_{m,c}$  increases nearly linearly with  $Pr$  and the variation rate of  $Ra_{m,c}$  gets larger when the Taylor number is increased. For each values of  $Ta$ , the magnetic Rayleigh number reaches the value  $Ra_{m,c} = 1614.7$  at the value of the Prandtl number close to  $Pr = 325$ . The value of  $Ra_{m,c} = 1614.7$  corresponds to the minimum of the marginal stability curve obtained for  $n = 0$  in the case where the inner cylinder is at rest ( $Ta = 0$ ). This minimum takes a slightly larger value than the critical one obtained for  $n = 13$ , but it is the reference from which the role played by rotation on the threshold of SA modes can be estimated. For  $Pr < 325$ , the rotation of the inner cylinder destabilizes the circular Couette flow since the magnetic Rayleigh number gets lower than its value in the absence of rotation and the larger the Taylor number is, the lower  $Ra_{m,c}$  becomes. However  $Ra_{m,c} > 1614.7$  for  $Pr > 325$  and the higher  $Ta$  is, the higher  $Ra_{m,c}$  gets, which indicates that the rotation now has a stabilizing role.

When the inner cylinder is hotter than the outer one, the thermomagnetic buoyancy destabilizes the flow, but the rotation of the inner cylinder intervenes in two competing mechanisms. On the one hand, the base azimuthal velocity profile exhibits a decrease of the angular momentum with the radial distance. Hence, the increase of the angular velocity of the inner cylinder destabilizes the circular Couette flow. On the other hand, the base azimuthal velocity produces a centrifugal acceleration which impacts the density stratification and tends to stabilize the flow. Figure 5(b)

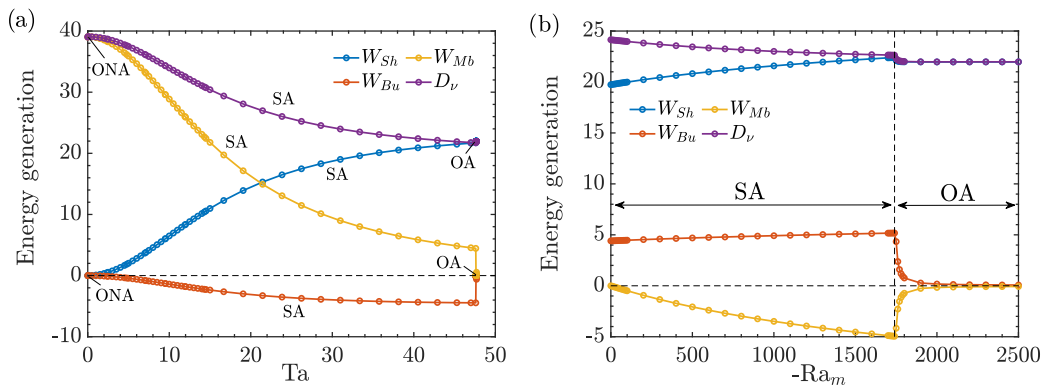


FIG. 6. Variation of the different terms in (15) for  $\eta = 0.8$  and  $Pr = 350$ . For  $\gamma_a = 0.01$  (a) the energy terms are plotted against  $Ta$  and for  $\gamma_a = -0.01$  (b) the energy terms are plotted against  $(-Ra_m)$ .

indicates that there exists a value of the Prandtl number above which the stabilizing effect of the centrifugal buoyancy overcomes the destabilizing mechanisms.

#### IV. ENERGY ANALYSIS

To get a better understanding of the role played by different driving forces intervening in the present flow, we computed their associated powers involved in the equation of the kinetic energy. The later is derived from the linearized equations of the perturbations. Multiplying Eqs. (13b)–(13d) by  $u'$ ,  $v'$ , and  $w'$ , respectively, and summing the resulting equations provides an equation describing the local energy transfer from the base state to the perturbed state around the marginal stability of the system. Integrating over a wavelength and over a period of the marginal perturbations results in

$$\frac{dK}{dt} = W_{Sh} + W_{Bu} + W_{Mb} - D_v, \quad (15)$$

where  $K$  is the kinetic energy,  $W_{Sh}$  is the power performed by the shear stress,  $W_{Bu}$  is the power performed by the centrifugal buoyancy,  $W_{Mb}$  is the power performed by the thermomagnetic buoyancy and  $D_v$  is the rate of viscous dissipation. These terms are given by

$$\begin{aligned} K &= \int \frac{\mathbf{u}'^2}{2} dV, \quad W_{Sh} = - \int u'v'r \frac{d\Omega}{dr} dV, \quad W_{Bu} = -\gamma_a \int u'(r\Omega^2\theta' + \Theta\Omega v')dV, \\ W_{Mb} &= \frac{Ra_m}{Pr} \int \theta'g_mu'dV, \quad D_v = \int \Phi_v dV, \end{aligned} \quad (16)$$

where the viscous dissipation function  $\Phi_v$  is given by

$$\begin{aligned} \Phi_v &= 2 \left[ \left| \frac{du'}{dr} \right|^2 + \left| \frac{imv'}{r} + \frac{u'}{r} \right|^2 + k^2|w'|^2 \right] + \left| r \frac{d}{dr} \left( \frac{v'}{r} \right) + \frac{imu'}{r} \right|^2 + \left| \frac{imw'}{r} + ikv' \right|^2 \\ &\quad + \left| iku' + \frac{dw}{dr} \right|^2. \end{aligned} \quad (17)$$

Each of these power terms are normalized using the kinetic energy so that they are comparable from one set of control parameters to another. In the following, these power terms are evaluated at the critical state, where the growth of kinetic energy vanishes. For outward heating [ $\gamma_a > 0$ , Fig. 6(a)],  $W_{Sh}$  and  $W_{Mb}$  are always positive while  $W_{Bu}$  is negative. This highlights the destabilizing contribution of the sheared flow and of the thermomagnetic buoyancy, and the stabilizing contribution of the centrifugal buoyancy. The thermomagnetic force is the leading mechanism for small values of

Ta. When Ta increases, the contribution of the thermomagnetic buoyancy diminishes while the destabilization by the shear flow increases. In contrast,  $W_{Bu}$  starts from zero at  $Ta = 0$  and decreases with Ta indicating an increase of the stabilizing mechanism. For SA modes, we always have  $W_{Mb} > -W_{Bu}$ . As soon as we have  $W_{Mb} = -W_{Bu}$ , the critical modes become oscillatory and the contribution of both mechanisms rapidly decreases with the decrease of  $Ra_m$  (see OA branch of [Fig. 3(a)]). For OA modes, the two power terms become negligible, which indicates that the two buoyancies are no longer contributing to the growth of perturbation kinetic energy. This mechanism following the excitation of oscillatory modes was also found by Yoshikawa *et al.* [44] in the case of a dielectric fluid subject to the dielectrophoretic force. In their case, the power performed by the thermoelectric buoyancy played the same role as the power performed by the thermomagnetic buoyancy in our case.

For inward heating [ $\gamma_a < 0$ , Fig. 6(b)], the shear flow still has a destabilizing effect since  $W_{Sh} > 0$ , but the role played by the thermomagnetic buoyancy and the centrifugal buoyancy are exchanged compared to the case where  $\gamma_a > 0$ . The centrifugal buoyancy destabilizes the flow since  $W_{Bu} > 0$  and the thermomagnetic buoyancy has a stabilizing effect with  $W_{Mb} < 0$ . When  $(-Ra_m)$  increases, the stabilizing effect of the thermomagnetic force increases. This is accompanied with the increase of the critical value of the Taylor number, which also increases  $W_{Sh}$  and  $W_{Bu}$ . The oscillatory modes occur at sufficiently large values of  $(-Ra_m)$  through a similar process than that observed for  $\gamma_a > 0$ . For SA modes, we have  $W_{Bu} > -W_{Mb}$ , but as soon as  $W_{Bu} = -W_{Mb}$ , the axisymmetric modes become oscillatory and both the centrifugal buoyancy and the thermomagnetic buoyancy see their contribution to the exchange of energy vanish for sufficiently large values of  $(-Ra_m)$ . In Fig. 7, the eigenfunctions computed at the critical state are shown for the OA modes encountered in inward heating. The temperature and the velocity field are shown in the first line while the energy density resulting from the centrifugal and the thermomagnetic buoyancy are shown in the second and third lines, respectively, together with their respective buoyancy fields  $\vec{b}'_c$  and  $\vec{b}'_m$  given by

$$\vec{b}'_c = -\frac{2\Theta V v' + V^2 \theta'}{r} \vec{e}_r, \quad \vec{b}'_m = \theta' g_m \vec{e}_r. \quad (18)$$

The density of energy of the centrifugal buoyancy and by the thermomagnetic buoyancy are given by

$$w_{Bu} = -\gamma_a u' (r \Omega^2 \theta' + \Theta \Omega v'), \quad w_{Mb} = \frac{Ra_m}{Pr} \theta' g_m u'. \quad (19)$$

At magnetic Rayleigh number  $(-Ra_m)$  taking its value just above the transition from SA to OA modes, the temperature and velocity field are in phase, meaning that hot fluids at the outer cylinder are transported to the inner cylinder passing through a hot area. Meanwhile, the cold fluid at the inner cylinder is transported toward the outer cylinder passing through a cold area. This mechanism induces zones where perturbations are excited by the centrifugal buoyancy, but damped by the thermomagnetic buoyancy. At larger values of  $(-Ra_m)$ , a phase difference between the radial velocity and the temperature appears and increases with the increase of  $(-Ra_m)$ . The phase delay induces the periodic appearance of zones with negative net product of  $\theta'$  and  $u'$ . Therefore the centrifugal buoyancy locally absorbs energy from the base state and tends to lower the overall power performed by this mechanism. In counterpart, the thermomagnetic buoyancy locally transfers energy to the perturbations and tends to increase  $W_{Mb}$ . In Fig. 7(e) obtained for  $Ra_m = -2500$ , the phase difference between  $u'$  and  $\theta'$  is close to  $\pi/2$ . In that case, the density of energy of both buoyancy mechanisms exhibits zones of positive and negative values with equivalent sizes and amplitudes, so that the spatial integration tends to vanish. As a result, the powers performed by the centrifugal buoyancy and by the thermomagnetic buoyancy tend towards zero. A similar result has been described by Meyer *et al.* [24] in the case of a nonisothermal Taylor-Couette system with the inner cylinder rotating.

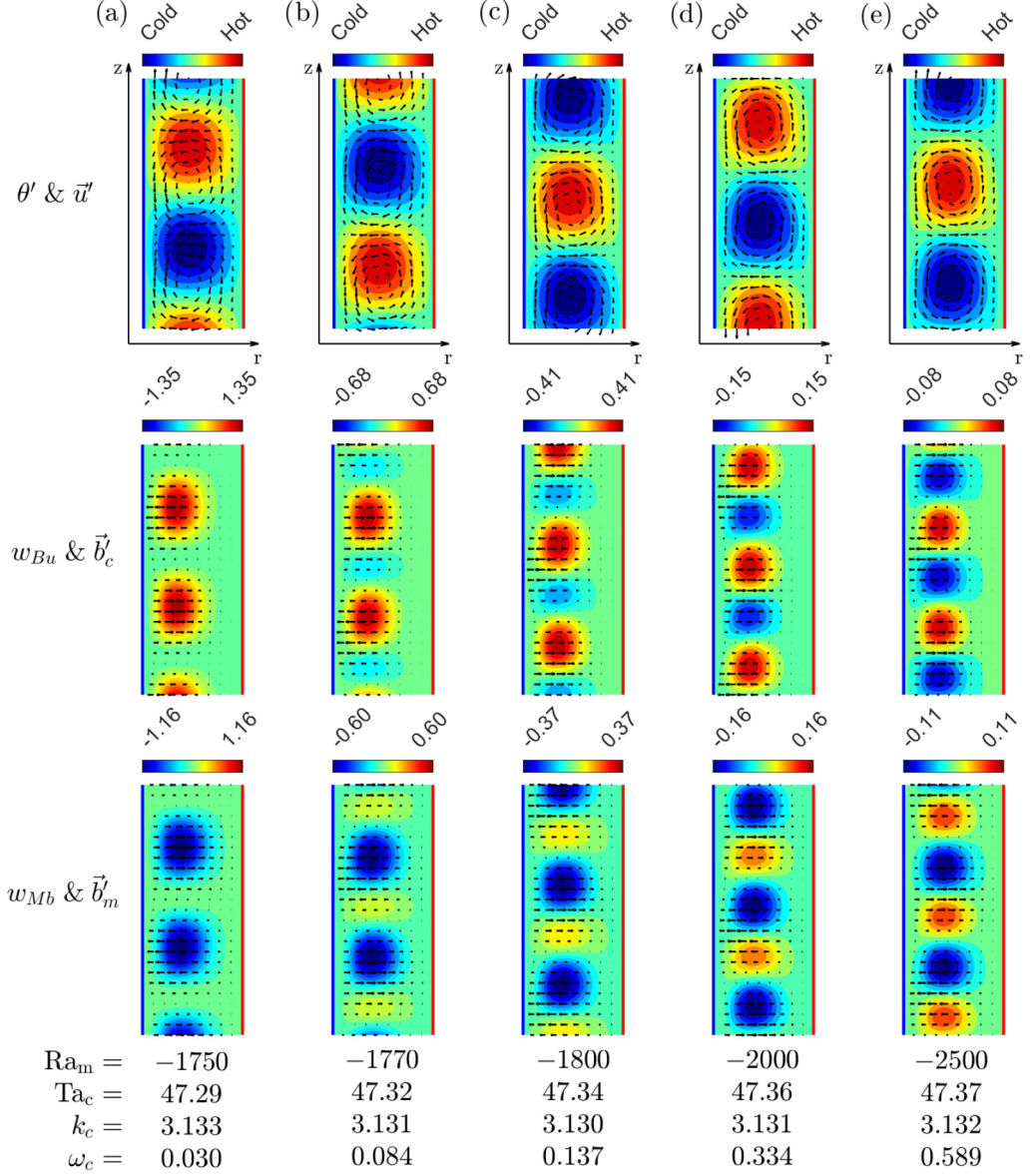


FIG. 7. Eigenfunctions plotted at the critical conditions for  $\eta = 0.8$ ,  $Pr = 350$ ,  $\gamma_a = -0.01$  and for different  $Ra_m$ . The first line shows the isosurface of perturbed temperature and the perturbed velocity field. The second line shows the isosurface of energy density produced by the centrifugal buoyancy and the centrifugal buoyancy field. The third line shows the isosurface of energy density produced by the thermomagnetic buoyancy and the thermomagnetic buoyancy field.

## V. LINEAR GINZBURG-LANDAU ANALYSIS

The Ginzburg-Landau equation describes the behavior of the amplitude  $A$  of a perturbation around the critical state. Considering axisymmetric modes, this equation is given by [45]

$$\tau_0 \left( \frac{\partial A}{\partial t} - c_g \frac{\partial A}{\partial z} \right) = \epsilon(1 - ic_0)A + \xi_0^2(1 - ic_1) \frac{\partial^2 A}{\partial z^2} - l(1 - ic_3)|A|^2 A + g(1 - ic_5)|A|^4 A. \quad (20)$$

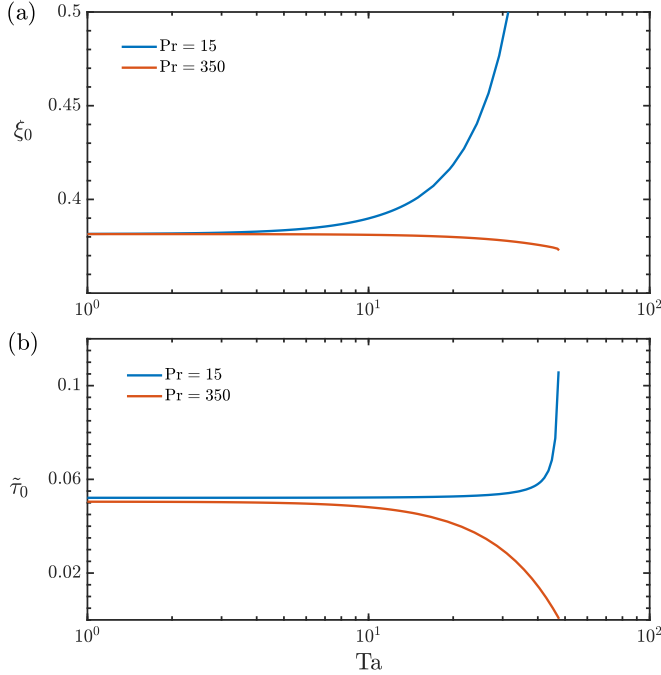


FIG. 8. Variation of (a) coherent length  $\xi_0$  and (b) the characteristic time divided by the Prandtl number  $\tilde{\tau}_0 = \tau_0/\text{Pr}$  as functions of  $Ta$  for the SA modes with  $\eta = 0.8$  and  $\gamma_a = 0.01$ .

The coefficients from the linear terms of Eq. (20) are calculated from the linear stability analysis in two different ways. Either  $Ra_m$  is fixed and the coefficient are evaluated around the critical Taylor number, or  $Ta$  is fixed and the magnetic Rayleigh number is varied around its critical value to determine the coefficients. The coefficients for the linear terms of Eq. (20) are given by

$$\begin{aligned} \epsilon &= \frac{\chi}{\chi_c} - 1; & \tau_0 &= \left( \chi_c \frac{\partial \sigma}{\partial \chi} \Big|_c \right)^{-1}; & \xi_0 &= \left[ - \frac{\partial^2 \sigma}{\partial k^2} \Big|_c / \left( 2 \chi_c \frac{\partial \sigma}{\partial \chi} \Big|_c \right) \right]^{1/2}; & c_g &= \frac{\partial \omega}{\partial k} \Big|_c; \\ c_0 &= \frac{\partial \omega}{\partial \chi} \Big|_c / \frac{\partial \sigma}{\partial \chi} \Big|_c; & c_1 &= \frac{\partial^2 \omega}{\partial k^2} \Big|_c / \frac{\partial^2 \sigma}{\partial k^2} \Big|_c, \end{aligned} \quad (21)$$

where  $\chi \equiv Ta$  when  $Ra_m$  is fixed and  $\chi \equiv Ra_m$  when  $Ta$  is fixed. The parameters  $\xi_0$  and  $\tau_0$  represent the coherent length and the characteristic time of the perturbation, respectively. They relate to the time and distance needed by the perturbation to reach the saturated state. The perturbation oscillation is characterized by the phase velocity  $c_z = \omega_c/k_c$  and the group velocity  $c_g$ , as well as the two coefficients  $c_0$  and  $c_1$ . The Landau constant  $l$  determines the nature of the bifurcation. If  $l > 0$  the bifurcation is supercritical, and one can see from Eq. (20) that for a stationary perturbation, the amplitude saturates at the equilibrium value  $A_e = \sqrt{\epsilon/l}$  after a long enough time. If  $l < 0$ , the bifurcation is subcritical and no saturation is expected, except if the fifth-order nonlinear term, i.e., the fourth term in the right-hand-side of Eq. (20), is taken into account. The coefficients  $l$ ,  $g$ ,  $c_3$ , and  $c_5$  cannot be extracted from the linear stability analysis, but they could be calculated through numerical simulations or weakly nonlinear analysis. We first analyze the SA modes encountered when  $\gamma_a > 0$  and plot the coherent length  $\xi_0$  [Fig. 8(a)] and the characteristic time normalized by the characteristic time of thermal diffusivity  $\tilde{\tau}_0 = \tau_0/\text{Pr}$  [Fig. 8(b)] as functions of  $Ta$ , the fixed parameter in that case. For small values of the Taylor number,  $\xi_0$  is independent of the Prandtl number and  $\tilde{\tau}_0$  is nearly independent of  $\text{Pr}$ . Both coefficients are increasing with the  $Ta$  for

TABLE I. Coefficients of the Guinzburg-Landau equation with fixing  $Ra_m$  with  $\eta = 0.8$  and for various parameters.

$\gamma_a = 0.01$										
Pr	$Ra_m$	$Ta_c$	$k_c$	$\omega_c$	$\tau_0$	$\xi_0$	$c_z$	$c_g$	$c_0$	$c_1$
15	479	40.79	3.131	0	0.186	0.323	0	0	0	0
350	479	47.65	3.131	0.7754	0.0759	0.2699	0.2477	0.2162	-0.0133	-0.0699
$\gamma_a = -0.01$										
Pr	$-Ra_m$	$Ta_c$	$k_c$	$\omega_c$	$\tau_0$	$\xi_0$	$c_z$	$c_g$	$c_0$	$c_1$
15	$10^2$	47.60	3.134	0	0.031	0.262	0	0	0	0
15	$10^3$	50.25	3.109	2.7078	0.070	0.268	0.8710	0.7231	-0.5635	-0.4015
350	$10^2$	33.81	3.150	0	4.015	0.259	0	0	0	0
350	$2 \cdot 10^3$	47.36	3.131	0.3343	0.075	0.269	0.1068	0.0800	-0.3682	-0.1637

Pr = 15 while they are decreasing with Ta for Pr = 350. This once again indicates the impact that the Prandtl number has on the role played by the centrifugal buoyancy. In practice, the occurrence of SA modes in a water-based ferrofluid would be disadvantaged by the increase of the rotation rate of the inner cylinder because of the finite length of the cylinders. However, in an oil-based ferrofluids with Pr = 350, the increase of the rotation rate of the inner cylinder favors the occurrence of the SA modes. Table I shows the values of the coefficients of the Ginzburg-Landau equation for the axisymmetric modes in outward and inward heating. Overall, we see that  $\xi_0$  weakly varies with Pr while  $\tau_0$  depends strongly on Pr. The OA modes exhibit normal dispersion since we have  $c_z > c_g$ .

## VI. CONCLUSION

The linear stability analysis of a ferrofluid confined between a rotating inner cylinder and a steady outer cylinder in the presence of a radial temperature gradient and a radially decreasing magnetic field has been performed. A water-based (Pr = 15) and an oil-based (Pr = 350) ferrofluid were investigated with the aim of evaluating the impact of the centrifugal buoyancy on the flow stability. For a water-based ferrofluid in outward heating, we obtained results which are similar to those obtained by Tagg and Weidman [16] when the magnetic gravity measured at the inner cylinder is 10 times larger than the Earth's gravity. The modes are helical for small rotation rates with a number of modes in the azimuthal direction which decreases with the increase of Ta until the modes become toroidal. In inward heating, the modes are axisymmetric and are found to be stationary for small magnetic Rayleigh numbers and oscillatory for larger ones. For this water-based ferrofluid, the effect of the centrifugal buoyancy is minor.

For an oil base ferrofluid, it is found that the centrifugal buoyancy has an important impact on the flow stability. In inward heating, the threshold between stable and unstable flow is obtained at lower values than for the water-based fluid. In outward heating, the stationary axisymmetric modes are stabilized by the increase of the rotation rate of the inner cylinder, which is counter-intuitive regarding the destabilizing mechanism of the angular momentum. In addition, oscillatory axisymmetric modes become critical at small values of  $Ra_m$  because of the stabilizing effect of the centrifugal buoyancy.

The energy analysis allows us to determine how important the different mechanisms for sustaining or damping of perturbations are. In addition to the global powers, the local energy densities performed by each force can be observed and efficiently serve to depict the cause of a change in the temporal nature of a critical mode.

The analysis using the linear Ginzburg-Landau equation highlighted the change of the role played by the inner cylinder rotation in outward heating depending on the Prandtl number. The coefficients of this equation are additionally given for different fluid properties and control parameters for possible future determination of an experimental setup.

## ACKNOWLEDGMENTS

The present work benefited from the financial support of the French Space Agency (Centre National d'Etudes Spatiales) and the French National Research Agency (Agence Nationale de la Recherche) through the program "Investissements d'Avenir" (ANR-10LABX-09-01) LABEX EMC<sup>3</sup> (project INFEMA) and the Regional Council of Normandy.

- 
- [1] M. D. Cowley and R. E. Rosensweig, The interfacial stability of a ferromagnetic fluid, *J. Fluid Mech.* **30**, 671 (1967).
  - [2] R. E. Rosensweig, Magnetic fluids, *Ann. Rev. Fluid Mech.* **19**, 437 (1987).
  - [3] R. E. Rosensweig, *Ferrohydrodynamics* (Cambridge University Press, Cambridge, 1985).
  - [4] M. I. Shliomis, Equations of motion of a fluid with hydromagnetic properties, *Sov. Phys. JETP* **26**, 665 (1968).
  - [5] M. I. Shliomis, Effective viscosity of magnetic suspensions, *Sov. Phys. JETP* **34**, 1291 (1972).
  - [6] A. Krekhov and M. Shliomis, Spontaneous Core Rotation in Ferrofluid Pipe Flow, *Phys. Rev. Lett.* **118**, 114503 (2017).
  - [7] A. N. Vislovich, V. A. Novikov, and A. K. Sinitsyn, Influence of a magnetic field on the Taylor instability in magnetic fluids, *J. Appl. Mech. Tech. Phys.* **27**, 72 (1986).
  - [8] P. J. Stiles, M. Kagan, and J. B. Hubbard, On the Couette-Taylor instability in ferrohydrodynamics, *J. Colloid Interface Sci.* **120**, 430 (1987).
  - [9] M. Niklas and H. Müller-Krumbhaar, Taylor-vortex flow of ferrofluids in the presence of general magnetic fields, *J. Magn. Magn. Mater.* **81**, 29 (1989).
  - [10] J. Singh and R. Bajaj, Couette flow in ferrofluids with magnetic field, *J. Magn. Magn. Mater.* **294**, 53 (2005).
  - [11] S. Altmeyer, Ch. Hoffmann, A. Leschhorn, and M. Lücke, Influence of homogeneous magnetic fields on the flow of a ferrofluid in the Taylor-Couette system, *Phys. Rev. E* **82**, 016321 (2010).
  - [12] B. A. Finlayson, Convective instability of ferromagnetic fluids, *J. Fluid Mech.* **40**, 753 (1970).
  - [13] P. J. Stiles and M. Kagan, Thermoconvective instability of a ferrofluid in a strong magnetic field, *J. Colloid Interface Sci.* **134**, 435 (1990).
  - [14] J. E. Hart, Ferromagnetic rotating Couette flow: the role of the magnetic viscosity, *J. Fluid Mech.* **453**, 21 (2002).
  - [15] R. Ganguly, S. Sen, and I. K. Puri, Thermomagnetic convection in a square enclosure using a line dipole, *Phys. Fluid* **16**, 2228 (2004).
  - [16] R. Tagg and P. D. Weidman, Linear stability of radially-heated circular Couette flow with simulated radial gravity, *Z. Angew. Math. Phys.* **58**, 431 (2007).
  - [17] S. A. Suslov, Thermomagnetic convection in a vertical layer of ferromagnetic fluid, *Phys. Fluids* **20**, 084101 (2008).
  - [18] P. B. Szabo and W.-G. Früh, The transition from natural convection to thermomagnetic convection of a magnetic fluid in a non-uniform magnetic field, *J. Magn. Magn. Mater* **447**, 116 (2018).
  - [19] M. Niklas, Influence of magnetic fields on Taylor vortex formation in magnetic fluids, *Z. Phys. B* **68**, 493 (1987).
  - [20] J. Walowit, S. Tsao, and R. C. Diprima, Stability of flow between arbitrarily spaced concentric cylindrical surfaces including the effect of a radial temperature gradient, *J. Appl. Mech.* **31**, 585 (1964).
  - [21] V. M. Soundalgekar, H. S. Takhar, and T. J. Smith, Effect of radial temperature gradient on the stability of viscous flow in an annulus with a rotating inner cylinder, *Warme und Stoffübertragung* **15**, 233 (1981).
  - [22] C. Kong and I. Liu, The stability of nonaxisymmetric circular Couette flow with a radial temperature gradient, *Phys. Fluids* **6**, 2617 (1994).
  - [23] C. Kang, A. Meyer, I. Mutabazi, and H. N. Yoshikawa, Radial buoyancy effects on momentum and heat transfer in a circular Couette flow, *Phys. Rev. Fluids* **2**, 053901 (2017).

- [24] A. Meyer, H. N. Yoshikawa, and I. Mutabazi, Effect of the radial buoyancy on a circular Couette flow, *Phys. Fluids* **27**, 114104 (2015).
- [25] S. Chandrasekhar, *Hydrodynamic and Hydromagnetic Stability* (Clarendon, London, 1961).
- [26] F. H. Busse, Thermal instabilities in rapidly rotating systems, *J. Fluid Mech.* **44**, 441 (1970).
- [27] M. Auer, F. H. Busse, and R. M. Clever, Three-dimensional convection driven by centrifugal buoyancy, *J. Fluid Mech.* **301**, 371 (1995).
- [28] C. Kang, A. Meyer, H. N. Yoshikawa, and I. Mutabazi, Numerical study of thermal convection induced by centrifugal buoyancy in a rotating cylindrical annulus, *Phys. Rev. Fluid* **4**, 043501 (2019).
- [29] P. J. Stiles and M. Kagan, Stability of cylindrical Couette flow of a radially polarised dielectric liquid in a radial temperature gradient, *Physica A* **197**, 583 (1993).
- [30] A. Meyer, H. N. Yoshikawa, and I. Mutabazi, Stability of Rayleigh-stable Couette flow between two differentially heated cylinders, *Phys. Rev. Fluids* **6**, 033905 (2021).
- [31] A. O. Kuzubov and O. I. Ivanova, Magnetic liquids for heat exchange, *J. Phys. III France* **4**, 1 (1994).
- [32] G. K. Auerhammer and H. R. Brand, Thermal convection in a rotating layer of a magnetic fluid, *Eur. Phys. J. B* **16**, 157 (2000).
- [33] J. Huang, D. D. Gray, and B. F. Edwards, Thermoconvective instability of paramagnetic fluids in a nonuniform magnetic field, *Phys. Rev. E* **57**, 5564 (1998).
- [34] C. B. Moler and G. W. Stewart, An algorithm for generalized matrix eigenvalue problems, *SIAM J. Numer. Anal.* **10**, 241 (1973).
- [35] V. K. Polevikov and V. E. Fertman, Investigation of heat transfer through a horizontal layer of a magnetic liquid for the cooling of cylindrical conductors with a current, *Magnitnaya Gidrodinamika* **1**, 415 (1977).
- [36] S. Odenbach, Microgravity experiments on thermomagnetic convection in magnetic fluids, *J. Magn. Magn. Mater* **149**, 155 (1995).
- [37] H. Morimoto, T. Meakawa, and M. Ishikawa, Linear stability analysis of magnetic Rayleigh-Bénard convection, *Adv. Space Res.* **22**, 1271 (1998).
- [38] A. Alonso, M. Net, and E. Knobloch, On the transition to columnar convection, *Phys. Fluids* **7**, 935 (1995).
- [39] A. Alonso, M. Net, I. Mercader, and E. Knobloch, Onset of convection in a rotating annulus with radial gravity and heating, *Fluid Dyn. Res.* **24**, 133 (1999).
- [40] D. Pino, I. Mercader, and M. Net, Thermal and inertial modes of convection in a rapidly rotating annulus, *Phys. Rev. E* **61**, 1507 (2000).
- [41] S. V. Malik, H. N. Yoshikawa, O. Crumeyrolle, and I. Mutabazi, Thermo-electro-hydrodynamic instabilities in a dielectric liquid under microgravity, *Acta Astronaut.* **81**, 563 (2012).
- [42] H. N. Yoshikawa, O. Crumeyrolle, and I. Mutabazi, Dielectrophoretic force-driven thermal convection in annular geometry, *Phys. Fluids* **25**, 024106 (2013).
- [43] V. Travnikov, O. Crumeyrolle, and I. Mutabazi, Numerical investigation of the heat transfer in cylindrical annulus with a dielectric fluid under microgravity, *Phys. Fluids* **27**, 054103 (2015).
- [44] H. N. Yoshikawa, A. Meyer, O. Crumeyrolle, and I. Mutabazi, Linear stability of a circular Couette flow under a radial thermoelectric body force, *Phys. Rev. E* **91**, 033003 (2015).
- [45] M. C. Cross and P. C. Hohenberg, Pattern formation outside of equilibrium, *Rev. Mod. Phys.* **65**, 851 (1993).